Future Change in Tropical-Cyclone Tracks as Demonstrated with a 20-km-mesh Atmospheric Global Circulation Model. -North Atlantic-

*Hiroyuki Murakami (AESTO / MRI), Bin Wang (University of Hawaii / IPRC), and Akio Kitoh (MRI)

himuraka@mri-jma.go.jp

1.Purpose

Future changes in tropical-cyclone (TC) tracks, affected by global warming, have not been well investigated. These changes as well as intensity changes are important for socioeconomic damage in the future. However, most studies used coarse resolution models (e.g. 60-120 km mesh) for multi-year climate simulations. The low resolution deteriorates not only TC structures and intensity, but also real distributions of TC tracks and genesis positions.

In this study, we conducted multi-year climate simulations with a 20km-mesh Meteorological Research Institute and Japan Meteorological Agency AGCM (MRI/JMA AGCM) in order to investigate future change in TC tracks over the North Atlantic. The projection periods are from 1979 to 2003 for a present day simulation (PD) and from 2075 to 2099 for a global warmed future simulation (GW), which is based on the IPCC A1B scenario.

2.Experimental design

a) 20km-mesh MRI/JMA AGCM

	20 km mesh global climate model
Horizontal Grids	1920x 960
Vertical Layers	60
Truncation Wave	TL959
Grid Spacing	20km
Top Layer Pressure	0.4hPa
Dynamical frame	Semi-Lagrangian scheme
Radiation Process	Shibata et al. (1999) Solar (every hour) Infrared (3 hourly)
Precipitation Process	Prognostic Arakawa-schubert (Randall and Pan, 1993), Large-scale condentation Prognostic cloud water content
Gravity wave drug	Iwasaki et al (1989)
Land surface	Simple Biosphere(SiB)
PBL and surface fluxes	Mellor-Yamada level 2 Moni-Obukhov similarity

b) Integration Periods

Present day (PD) : 1979-2003 (25 years)

Future (GW): 2075-2099 (25 years)

c) Lower Boundary Conditions (SST & Sea Ice Concentration)

For PD run:
The Hadley Centre Sea-Ice and Sea-Surface Temperature data set version 1 (HadISST1) is directly used.

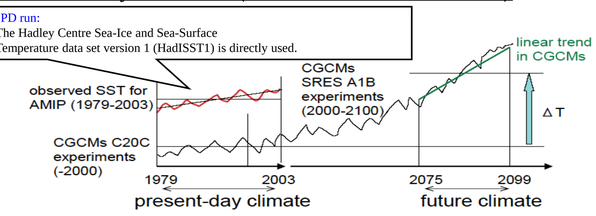

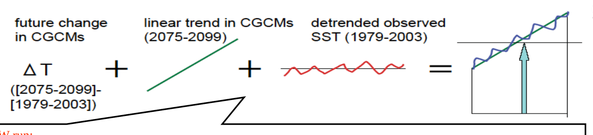

For GW run:
Linear trend and mean future change of SST and sea ice are decomposed by the CMIP3 multi-model ensemble mean simulations based on IPCC SRES A1B scenario. Interannual variation by observation is also decomposed. These trend, mean future change, and interannual variation are reconstructed for future boundary conditions .

FIG. 1 Schematic diagram of prescribed future SST and sea ice concentration.

d) Detection method for TCs

The method for TC identification involves the six sets of criteria described in Oouchi et al.(2006) as follows.

1. The minimum surface pressure is at least 2 hPa lower than the surrounding 7 degree x 7 degree grid box.
2. The magnitude of the maximum relative vorticity at 850hPa exceeds 3.5 x 10^(-5) /s
3. The maximum wind speed at 850 hPa is larger than 12m/s,
4. The sum of the temperature deviations at 300, 500 and 700hPa exceeds 1.2 K for warm core.
5. The maximum wind speed at 850 hPa (WS850) exceeds that at 300 hPa (WS300) at the first detection (i.e., generation time) of a TC. After generation, WS850 added by 2.5 m/s should be greater than WS300.
6. The duration is not shorter than 36 hours.

e) Observation data

a) Best Tracks

A global TC best-track data provided by Unisys Corporation Website (http://weather.unisys.com/hurricane)

b) JRA-25 reanalysis data

The JRA-25 reanalysis dataset (Onogi et al. 2007) was used for GPI analysis. The JRA-25 reanalysis system was constructed based on the former global operational forecast and assimilation system at the JMA.

3. Overall result of simulated TC frequency for each basin

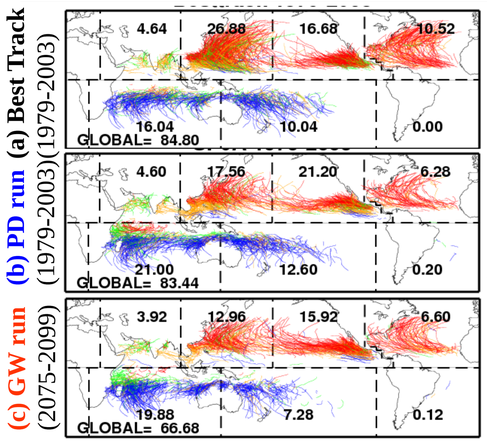

TAB.1 Statistics of annual mean TC numbers for each simulation.

Region	Observation	PD	GW	GW−PD
Global	84.80	83.44	66.68	−16.76
N.Hemisphere	58.72	49.64	39.36	−10.28
S.Hemisphere	26.08	33.76	27.24	−6.52
North Indian	4.68	4.60	3.92	−0.68
western North Pacific	26.84	17.56	12.96	−4.60
eastern North Pacific	16.68	21.20	15.88	−5.32
North Atlantic	10.52	6.28	6.60	0.32
South Indian	16.04	21.00	19.84	−1.16

#Green columns mean 99% statistical significance for the future difference.

Reductions in TC frequency are seen for the most basins except for the North Atlantic.

FIG. 2 All tracks for (a) Best track, (b) PD run, and (c) GW run. Colors mean TC tracks for each season of JFM (Blue), AMJ (Green) , JAS (Red), and OND (Orange). Numbers mean annual averaged TC number.

4. Track change over the North Atlantic

Change in tracks

(a) PD run (TC tracks, 1979-2003, JASO)

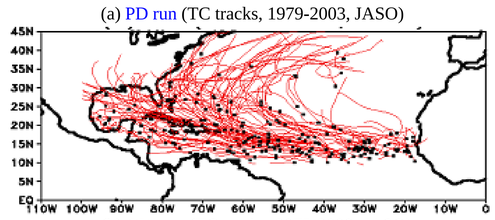

(b) GW run (TC tracks, 2075-2099, JASO)

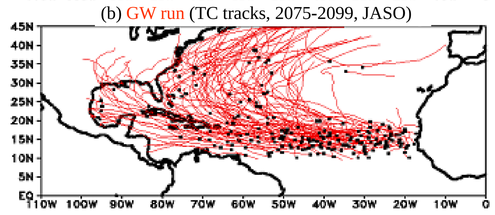

(c) GW - PD (frequency of TC occurrence, JASO)

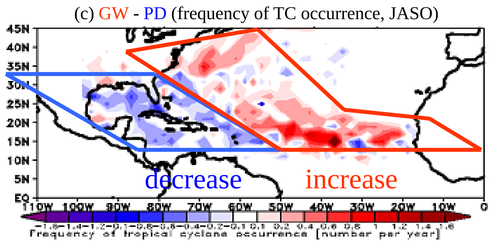

FIG. 3 Total TC tracks over North Atlantic in July-Ougust for (a) PD, and (b) GW run. Difference in frequency of occurrence is shown in (c).

TC tracks show a significant eastward shift in future, resulting in a reduced probability of TC landfall over North America.

Change in large-scale flow

(a) PD run (1979-2003, JASO)

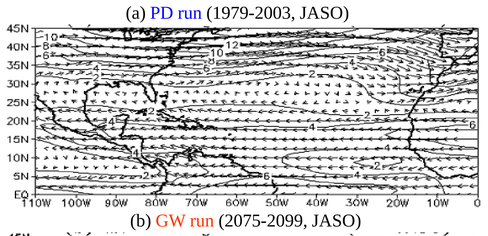

(b) GW run (2075-2099, JASO)

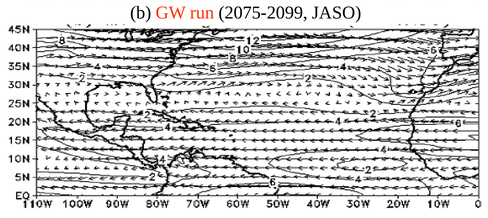

(c) GW - PD (JASO)

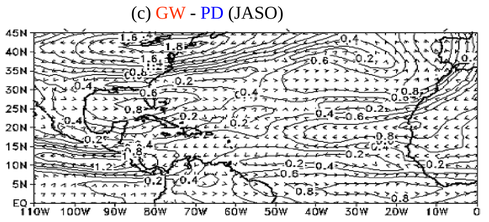

FIG. 4 Simulated large-scale steering flows (m/s) for the peak cyclone season of July–October (JASO) for (a) the PD run, (b) the GW run, and (c) the difference between the GW and PD runs. Large-scale steering flows were defined as pressure-weighted mean flows from 850 to 300 hPa

Change in large-scale flow does not explain TC track changes.

Change in frequency of TC genesis

(a) PD run (1979-2003, JASO)

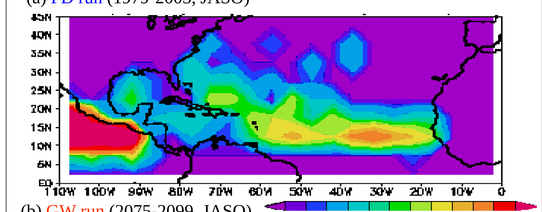

(b) GW run (2075-2099, JASO)

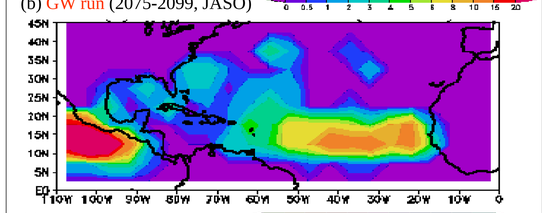

(c) GW - PD (JASO)

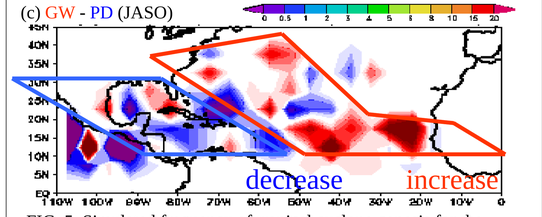

FIG. 5 Simulated frequency of tropical cyclone genesis for the peak cyclone season of July–October (JASO) for (a) the PD run, (b) the GW run, and (c) the difference between the GW and PD runs.

These changes appear to be consistent with the predicted change in frequency of TC occurrence (Fig. 3c), thereby indicating that the change is caused mainly by the change in frequency of genesis.

Why did TC tracks shift eastward? → Large-scale flow changed? ***NO*** → Genesis locations changed? ***YES***

5. Emanuel and Nolan's Genesis Potential Index (GPI) wish some modifications

To determine the factors behind such genesis changes, we used a Genesis Potential Index (GPI). The GPI was originally developed by Emanuel and Nolan (2004), motivated by the work of Gray (1979). The formulation is as follows:

$$GPI = \left|10^5 \eta\right|^{\frac{3}{2}} \left(\frac{RH}{50}\right)^3 \left(\frac{V_{pt}}{70}\right)^3 \left(1+0.1V_s\right)^{-2}, \qquad (1)$$

where η is the absolute vorticity (s^{-1}) at 850 hPa, RH is the relative humidity (%) at 700 hPa, V_{pt} is the maximum potential intensity (m/s) of Emanuel (1995), and V_s is the magnitude of the vertical wind shear (m/s) between 850 and 200 hPa.

However, we found that when the GPI is applied to reanalysis data (or AGCM outputs), the original GPI has significant discrepancies with the observed (detected) distribution of TC genesis. In the present study, we modified the original GPI by explicitly by incorporating the following vertical motion term:

$$GPI' = \left|10^5 \eta\right|^{\frac{3}{2}} \left(\frac{RH}{50}\right)^3 \left(\frac{V_{pt}}{70}\right)^3 \left(1+0.1V_s\right)^{-2} \left(\frac{-\omega+0.1}{0.1}\right), \qquad (2)$$

where ω is the vertical wind velocity ($Pa \cdot s^{-1}$) at 500 hPa.

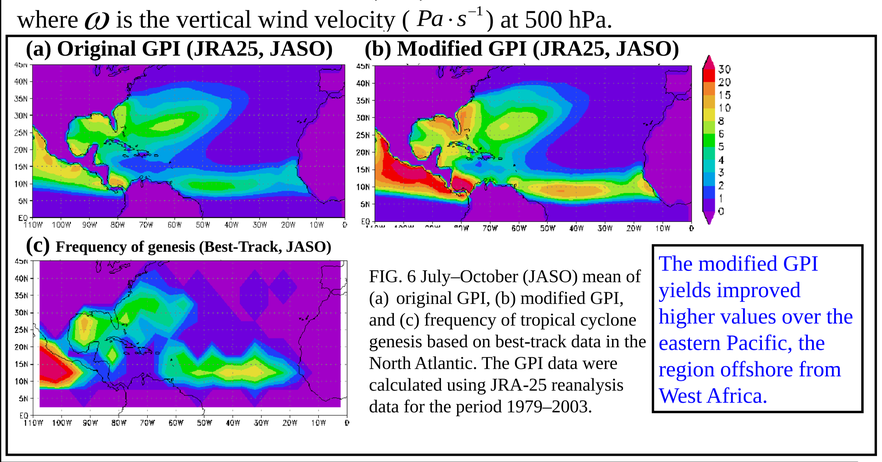

FIG. 6 July–October (JASO) mean of (a) original GPI, (b) modified GPI, and (c) frequency of tropical cyclone genesis based on best-track data in the North Atlantic. The GPI data were calculated using JRA-25 reanalysis data for the period 1979–2003.

The modified GPI yields improved higher values over the eastern Pacific, the region offshore from West Africa.

6. Reasons for future change in genesis location

a) GPI analysis

Above, we found that future changes in the frequency of TC occurrence arise from changes in the frequency of genesis rather than changes in large-scale flows. Here, we investigate the reason for such changes in frequency of genesis, based on the modified GPI.

The GPI can be used to determine which of the GPI elements contribute most to its future change. Here, we assign the future value to one of the five GPI elements in Eq. (2); the other elements are kept at the present-day values, as used in the PD run. The virtual GPI value is then subtracted from the present-day GPI value. In the case of a large difference, the assigned GPI element is considered an influential factor in terms of GPI change.

It is clear that changes in the maximum potential intensity and omega terms make the dominant contribution to the increase in the GPI within the eastern North Atlantic, whereas the relative humidity and omega terms make the largest contribution to the decrease in the GPI within the western North Atlantic.

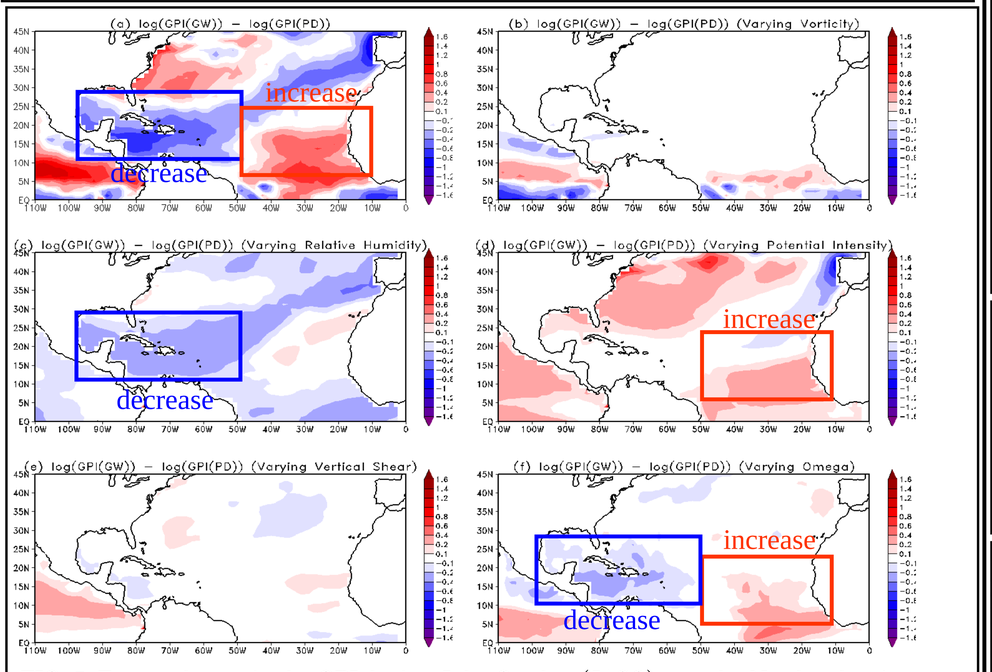

FIG. 7. Future change in the GPI during July–October (JASO) over the North Atlantic for (a) non-varying GPI (i.e., difference in GPI between the GW and PD runs), and for GPI changes obtained by varying (b) vorticity, (c) relative humidity, (d) maximum potential intensity, (e) vertical shear, and (f) omega, where in each case the other variables were those of the PD run. Gray shading indicates positive values.

b) Eastern North Atlantic

The GPI increase in the eastern NA is largely due to change in large-scale vertical motion and maximum potential intensity, which appear to be related to enhanced convective activity in the ITCZ. Figure 8 shows changes in July-October mean vertical velocity at 500 hPa in the NA. It is clear that upward motions are enhanced in the region offshore from West Africa. These changes are consistent with a predicted increase in precipitation (Fig. 9). In addition, prescribed future SST (Fig.10) is relatively higher at the eastern North Atlantic. Overall, these favorable environmental conditions for convective activity promote TC genesis near the eastern Atlantic ITCZ.

c) Western North Atlantic

In contrast to the findings for eastern NA, increased subsidence (Fig. 8c), decreased relative humidity, and reduced precipitation (Fig. 9c) can be seen in the western NA. The increase in vertical motions in the eastern NA and eastern Pacific acts to enhance zonal circulation, which results in turn in the suppression of convective activity over the western NA.

Note that precipitation is reduced in the western NA (Fig. 9c) despite an increase in SST (Fig. 10c). The distribution of the SST anomaly is important not only for local TC genesis, but also for remote TC genesis in the NA.

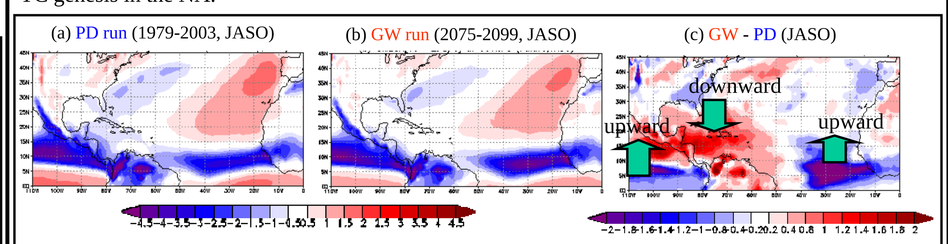

FIG. 8 Vertical velocity at 500 hPa for the peak cyclone season of July–October (JASO) for (a) the PD run, (b) the GW run, and (c) the difference between the GW and PD runs. Unit is 10^-2 Pa/s.

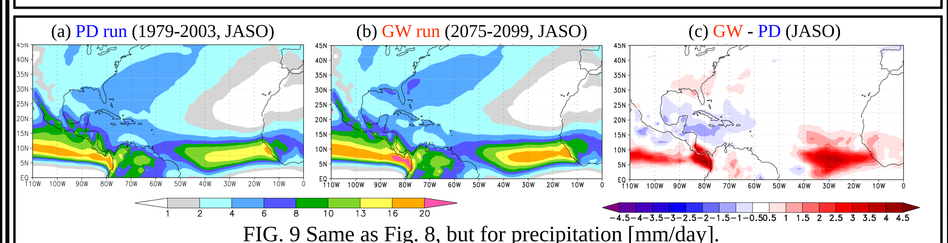

FIG. 9 Same as Fig. 8, but for precipitation [mm/day].

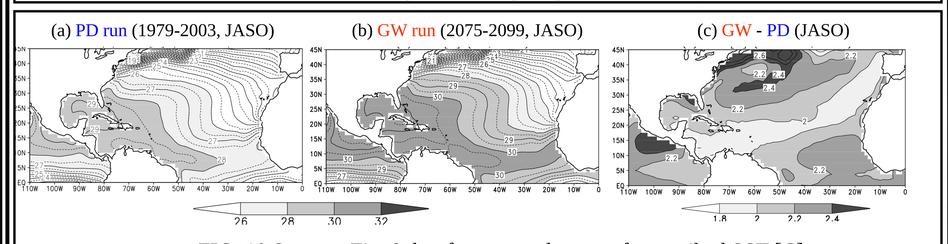

FIG. 10 Same as Fig. 8, but for seasonal mean of prescribed SST [C].

7. Conclusion

We conducted a pair of 25-year climate simulations for the present day (1979–2003, PD) and the last quarter of the 21st century (2075–2099, GW), based on the A1B scenario using a MRI/JMA 20-km-mesh high-resolution atmospheric general circulation model. The analysis focused on tropical cyclone (TC) activity, especially TC tracks, over the North Atlantic (NA).

Concerning future change, the change in frequency of TC occurrence was spatially inhomogeneous, with a marked decrease in the western NA and an increase in the eastern NA. A comparison of large-scale flows between the PD and GW runs reveals no significant change. In contrast, we found a marked change in the locations of TC genesis between the PD and GW runs; therefore, change of genesis locations is the major reason for the predicted change in frequency of occurrence and TC tracks.

The signal of TC location shifts is well captured by Emanuel and Nolan's Genesis Potential Index (GPI) change. The main factors contributing to the predicted future increase in TC genesis in the eastern NA were changes in maximum potential intensity and vertical motion, which are related to the enhanced convective activity in the eastern Atlantic ITCZ. The decrease in TC genesis in the western NA was related mainly to reduced relative humidity and increased subsidence. Although, the prescribed sea surface temperature (SST) showed increase in the western NA, convective activities were decreased by the unfavorable environmental factors. It is inferred that the increase in convective activity in the eastern NA or in the eastern Pacific was sufficiently large to result in enhanced Hadley circulation in the NA. In turn, this led to a subsidence anomaly over the western NA, which suppressed convective activity and resulted in a decrease in TC genesis over this region.